JISSS, 4(1), pp. 61–69, March–September 2015.

REGULAR PAPER

Complete development of a single cell PMUT transducer: design, fabrication, characterization, and integration

Ajay Dangi[a,*], Amod Hulge[b], Anish Somasundaran[c], Rominus S. Valsalam[c], Rudra Pratap[a,b]

[a]Department of Mechanical Engineering, IISc Bangalore, India

[b]Center for Nano Science and Engineering, IISc Bangalore, India

[c]Center for Development of Advanced Computing (C-DAC), Trivendrum, India

*Corresponding author: dangi.ajay@gmail.com; ajayd@mecheng.iisc.ernet.in

Keywords

Ultrasonic
Piezoelectric
PMUT
MEMS

Received: 07-10-2014
Revised: 26-11-2015
Accepted: 06-01-2016

Abstract

Microfabricated ultrasonic sensors have opened new avenues for sensor applications from emerging consumer electronics to conventional medical imaging. This work reports design, fabrication, and electronic integration of a Piezoelectric Micromachined Ultrasonic Transducer (PMUT). PMUT cells have been fabricated by suspending a multilayer structure on silicon substrate consisting mainly of a passive base layer and an electronically excitable piezoelectric layer. In the reported design, the PMUT uses 1 µm-thick PZT as piezoelectric layer with top and bottom electrodes on 300 nm-thick SiO_2 released after etching silicon handle layer of about ~525 µm thickness. Fabricated PMUT devices have been characterized using Laser Doppler Vibrometry (LDV) in transmitter and receiver modes. Further, the PMUT has also been integrated with electronics and a single 1 mm diameter PMUT has been shown to work as a proximity sensor up to 10 cm distance.

1 Introduction

Ultrasonic sensors are well known for various applications such as Non-destructive Testing, ultrasound imaging, and proximity sensing. Ultrasonic imaging based applications typically use an array of ultrasonic transducers which form an electronically steerable beam for scanning an area. Since the advent of micro-fabrication techniques for Micro-electro-mechanical Systems, development of ultrasonic sensors on silicon wafers, which promise to be smaller, Complementary metaloxide-semiconductor or CMOS integrable, and more energy efficient, has been an active area of research [Khuri-Yakub *et al.* 1998; Yamashita *et al.* 2002]. These microscale versions of ultrasonic sensors are known as Micromachined Ultrasonic Transducers or MUTs and they have two prominent variants based on their actuating principles: Capacitive MUTs and Piezoelectric MUTs, also aptly called CMUTs and PMUTs. The key component of a MUT is a suspended plate or membrane that vibrates in a flexural mode to generate sound. Hence, the transducer is directly coupled with the fluid medium. Because of the small size of the device, the structural dissipation becomes very small as compared to acoustic dissipation resulting in highly efficient conversion

Table 1. Comparison of conventional and MEMS ultrasonic sensors.

Type	A conventional ultrasonic sensor	MEMS ultrasonic sensor
Diameter	$\Phi = 10$ mm	$\Phi = 1$ mm
Operating voltage	10–30 V	1–5 V
Frequency	40 kHz	75 kHz
Acoustic output	119 dB	69.6 dB
Picture		

from electrical energy to acoustic energy. A comparison between a typical conventional ultrasonic sensor and a micromachined ultrasonic sensor is presented in Table 1.

Since the basic principles involved in integration and operation of conventional ultrasonic sensors and micromachined ultrasonic sensors are the same, the key challenge involved in the development of this technology is realising a single cell/element of a MUT, which is being presented in this paper.

Unlike CMUTs, PMUTs do not require high bias voltage and suspended membranes with very small gap [Khuri-Yakub *et al*. 1998]. This makes the fabrication process and device integration easy. However, development of a reliable piezoelectric thin film is a major challenge for PMUTs. We have used commercially available PZT coated wafers for fabrication. PZT is preferred over other piezoelectric materials for MEMS applications because of its high coupling coefficients.

2 Device architecture

We have used a circular unimorph structure with 1 mm diameter for the PMUT. The stack of layers in the PMUT includes 300 nm-thick SiO_2 as the passive base layer and 1 µm-thick PZT as the active piezoelectric layer (Figure 1). The 160 nm-thick Pt/Ti layer below PZT and the 160 nm Au/Cr layer above it are used as the bottom and top electrodes for the device, respectively.

On application of alternating voltage across the PZT film, the out-of-plane electric field generates in-plane stresses in the PZT layer. This excess stress is not symmetric with respect to the neutral

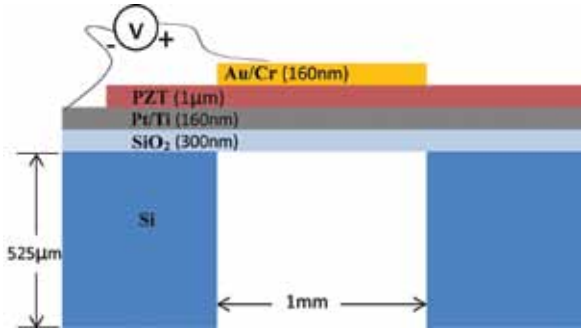

Figure 1. Cross-section view of PMUT.

plane of the structure, and therefore, it causes a net bending moment about the neutral plane. Hence, the suspended unimorph or the PMUT vibrates in the out-of-plane mode when a sinusoidal voltage input is applied across the piezoelectric layer. The vibrating unimorph pushes the air to generate an ultrasonic signal in the transmitter mode. Conversely, when an acoustic signal at the resonance frequency impinges on the unimorph, it vibrates and because of the piezoelectric effect, a potential difference develops across the piezoelectric layer.

The maximum deflection in the diaphragm for a given voltage input is generated when the ratio of the diameter of the top electrode to that of the bottom electrode lies between 0.6–0.9 [Bu Minqiang *et al*. 2003]. In our design, this ratio has been kept as 0.8. We have fabricated an array of 6×6 PMUTs on a 1.5 cm $\times$ 1.5 cm sample.

3 Fabrication

This section describes the main steps followed for fabrication of the PMUTs. The fabrication process starts with a commercially available 4 inch wafer with 300 nm-thick thermally grown SiO_2 layer, 160 nm sputtered Pt/Ti and 1 µm-thick PZT film deposited by sol-gel method (Figure 2-a). Pt/Ti layer acts as the bottom electrode for all the devices on one wafer piece. For the top electrode, 10 nm Cr and 150 nm Au layers are coated by sputtering and patterned using standard lift-off process (Figure 2-c). Backside mask is developed by photolithography after alignment of the backside photoresist mask with the top-side electrode pattern (Figure 2-d). Backside mask is used for anisotropic etching of SiO_2 using reactive ion etching (RIE) with CHF_3 chemistry (Figure 2-e). The SiO_2 pattern thus generated is used as a mask for the deep reactive ion etching (DRIE) of Si.

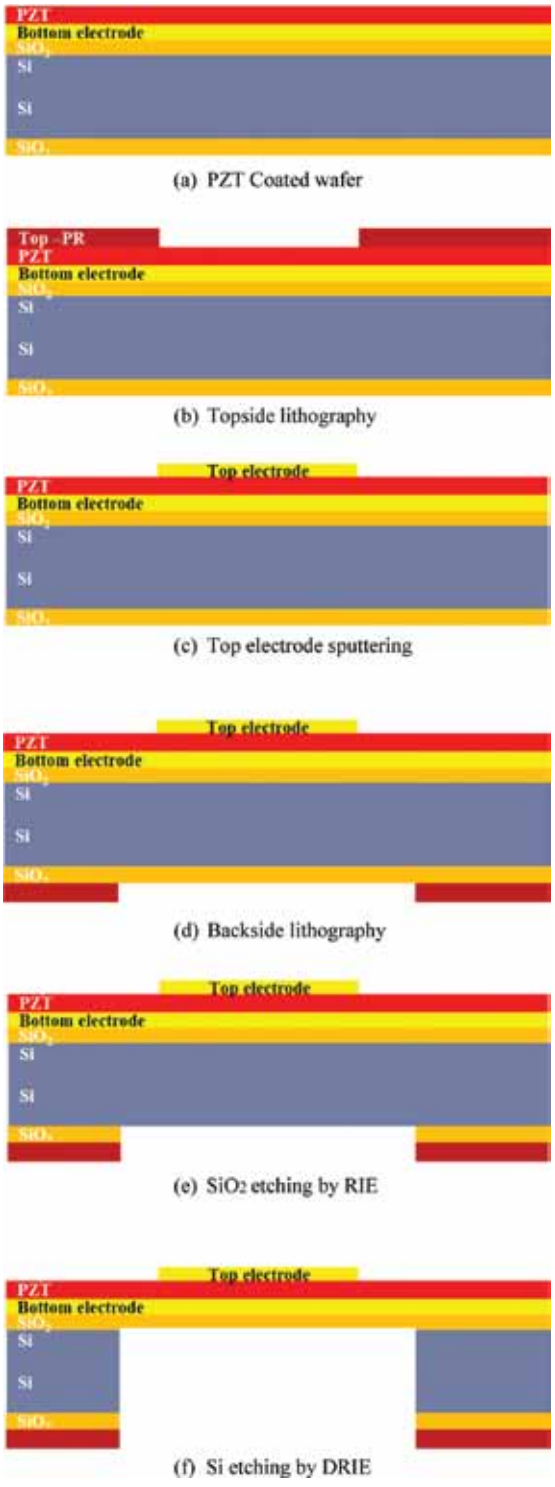

Figure 2. Steps involved in the fabrication of the PMUTs.

An optimized DRIE process is used to vertically etch 525 µm of Si, leaving behind 1.62 µm thick suspended unimorph structure (Figure 2-f). SiO_2 layer on the top side of the silicon layer acts as an etch stop for the DRIE etching step.

Figure 3. Si Grass formation during DRIE.

Fabrication of MEMS devices in any research facility usually takes up several runs even if the process sequence is already known. Unoptimised process parameters and the sensitivity of various processes to small changes in these parameters usually play truant in the realization of the final structure. We have had our own share of these problems that we resolved one by one. One of the major problem is Si grass formation [Dixit and Miano, 2006]. This problem was observed during the first few fabrication runs (Figure 3). Si grass formation may be caused by incomplete etching of SiO_2 and the presence of polymer particles on the mask window created before the Deep Reactive Ion Etching (DRIE) etching step. This problem was resolved by increasing etching duration of the RIE step. Cross-sectional SEM of the suspended membrane shows successful release of the devices without any severe damage to the SiO_2 layer (Figure 4). Since our devices have been fabricated on 1.5 cm × 1.5 cm substrate pieces, backside alignment is very challenging on standard mask alignment and exposure tool. We had to align the substrate to the mask by looking only through one lens and moving the substrate sideways multiple times to get the correct alignment.

The final devices were glued to a PCB patterned with gold pads. The devices on the wafer

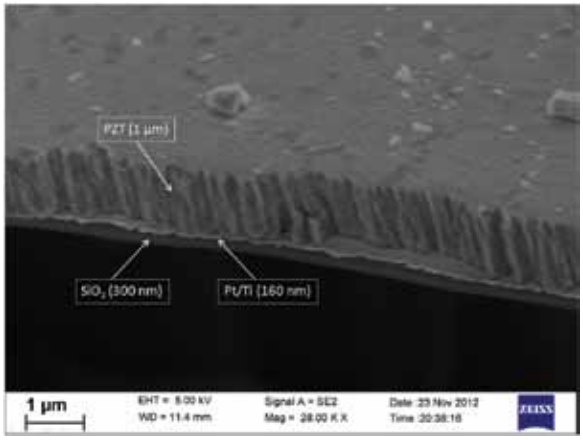

Figure 4. Cross-sectional SEM of a suspended PMUT.

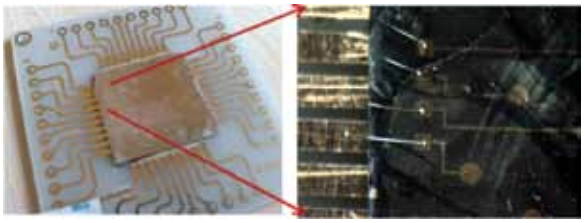

Figure 5. PMUT: Wire Bonding.

were then connected to the PCB pads using Al wires by the ultrasonic wire bonding technique (Figure 5).

4 Device characterization

4.1 *Vibrational characteristics*

The vibrational behaviour of the PMUT has been captured using Laser Doppler vibrometry (MSA 500) (Figure 6). The first resonance of the PMUT devices occurs between 72–78 kHz. The variation in natural frequencies of PMUTs is attributed to over-etching of SiO_2 and non-perpendicular landing of silicon etch on SiO_2 at the end of the DRIE etch step.

In order to obtain the damping factor and the amplitude of vibration, the response has been recorded at the center of the PMUT in a 10 kHz frequency band around the first resonance at different voltages from 0.5 V to 2 V using peak hold method (Figure 7).

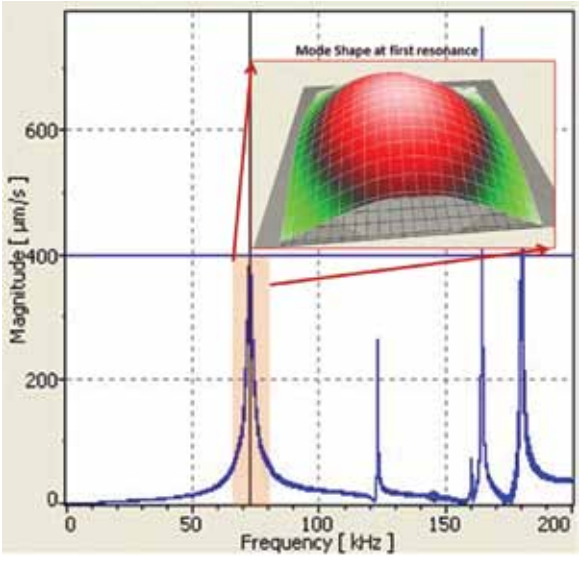

Figure 6. Frequency response of the PMUT. The inset shows the mode shape at the first peak.

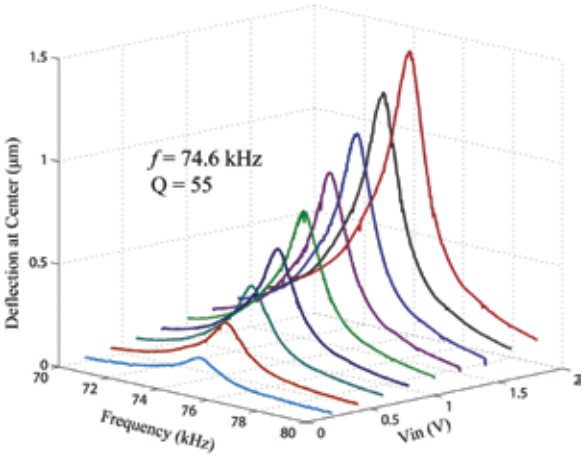

Figure 7. Frequency response of the PMUT for several (increasing) values of the input voltage from 0.2 V to 1.8 V (in 0.2 V increments).

For the method used, the frequency of the input voltage signal was swept very slowly from 70 kHz–80 kHz in approximately 10 s, while recording the peak amplitude in 32 ms time windows during the capture time. The quality factor, Q, has been found to be approximately 55, by using half power band method on the least square fit of the frequency response.

4.2 *Transmitter characteristics*

In order to establish the transmitter characteristics of the PMUT, the deflection at the center of the membrane has been plotted for different voltage inputs. The linear fit of the experimental data shows that the deflection sensitivity of the PMUT is approximately 805 nm/V (Figure 8).

Response of strain in a piezoelectric material to cyclically varying large electric field beyond the coercive field of the material shows a butterfly shaped curve (also known as butterfly loop) due to combined effect of hysteresis and domain switching [Damjanovic *et al*. 2005].

The slope of the upper arm of the butterfly loop is representative of deflection sensitivity of the PMUT in static loading condition for small voltages. We have captured the butterfly loop for the suspended PMUT using a commercial piezoelectric coefficient measurement system (Figure 9). Using the deflection for static loading case, the sensitivity of the transmitter at resonance can be estimated using the following equation.

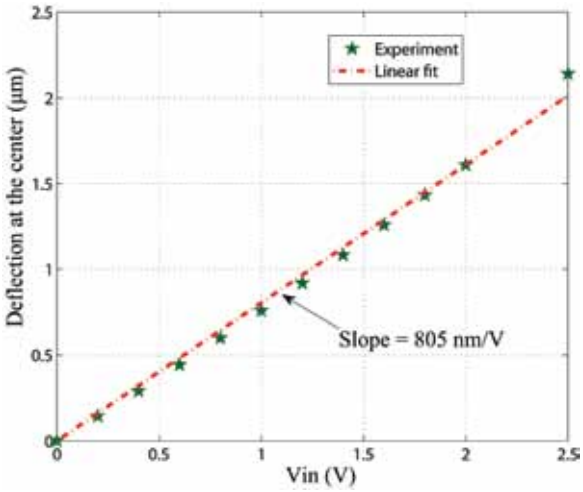

Figure 8. Centre deflection of a PMUT transmitter in response to the input voltage at its first resonance.

$$x_{resonance} = \frac{x_{static}}{2\zeta} = 605 \text{ nm/V} \qquad (1)$$

The quality factor and the deflection sensitivity of our PMUT sensors have been observed to vary between 35–80 and 200 nm/V to 900 nm/V respectively. This variability can be caused by misalignment of the top electrode, variability in actual diameter of the suspended membrane and acoustic radiation conditions on both sides of the membrane. Assuming that the PMUT is equivalent to a piston in a baffle displacing the same volume of air as the PMUT, the far field pressure can be evaluated by using

$$p(r,\theta,t) = \frac{j}{2}\rho_o C U_o \frac{a}{r} ka \left[\frac{2J_1(ka\sin\theta)}{ka\sin\theta}\right] e^{j(\omega t - kr)} \qquad (2)$$

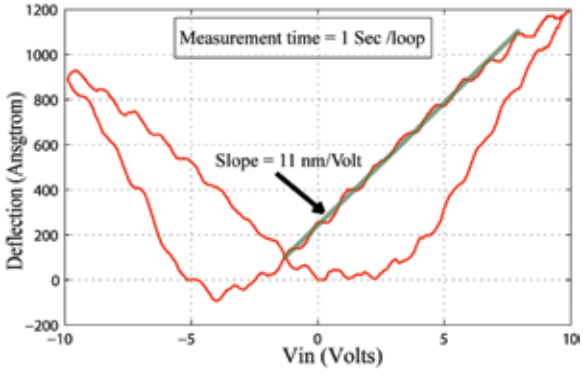

Figure 9. Butterfly loop showing d31 measurement on a suspended PMUT membrane.

Table 2. Analytical and experimentally observed transmitter pressure.

Deflection (μm)	**Measured P_{tx} (Pa)**	**Analytical P_{tx} (Pa)**
0.934	0.340	0.362
1.750	0.617	0.678
2.345	0.854	0.909
2.945	1.032	1.141
3.717	1.329	1.441

where J_1 is the Bessels function of the first kind, ρ_o is the density of air, C is the velocity of sound in air, U_o is the average velocity amplitude of the transducer, a is the radius of the transducer, k is the wavenumber, and ω is the operating frequency [Kinsler *et al*. 2000]. We have measured the acoustic pressure generated by the PMUT at approximately 3.5 cm distance using a wideband microphone (B&K 4138). The deflection of the transmitter, measured pressure and expected pressure are presented in Table 2 for a PMUT actuated at its first resonance.

Using equation (2) we get the pressure output per volt input at 1 meter distance from the PMUT as approximately 14.3 mPa/Volt or 57 dB. A general purpose ultrasonic sensor (Murata MA40S4R/S) can generate 119 dB sound pressure at 30 cm distance when actuated at 10 V. For the same conditions the PMUT can generate 87 dB sound pressure. The relatively small acoustic pressure of PMUT is because its area of radiation is approximately 100 times smaller than that of the conventional ultrasonic transducer.

4.3 *Receiver characteristics*

Similar to the transmitter, behaviour of the PMUT as a receiver has been studied for deflection sensitivity to acoustic input at resonance.

For these studies, a macro scale ultrasonic transmitter was kept at a known distance from the receiver and actuated electrically while receiver was probed by the LDV laser (Figure 10).

The voltage signal generated by the LDV was fed to the transmitter which in response generated acoustic output. This acoustic signal caused vibrations in the PMUT receiver which were captured by the LDV. A scan of the receiver membrane showed that it was only the suspended membrane area of the receiver die that vibrated

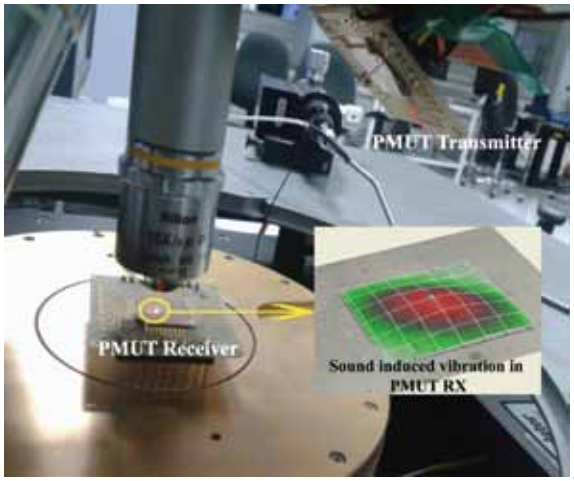

Figure 10. Setup for LDV characterization of a PMUT as receiver in response to another PMUT acting as transmitter.

significantly due to the acoustic input from the transmitter. The receiver deflection shows a linear response against the input acoustic pressure and the sensitivity of the deflection at the center of the PMUT to the acoustic input is approximately 11.3 nm/Pa (Figure 11).

5 Electronic integration and proximity sensing

It was observed that the voltage output generated by a single PMUT cell in response to the acoustic input provided by a macro transmitter or another

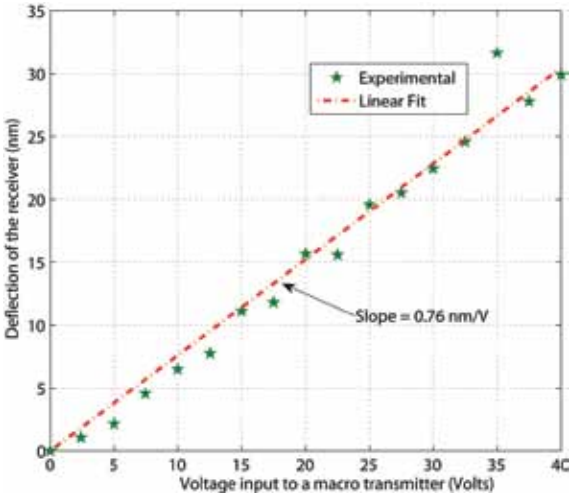

Figure 11. Centre deflection of a PMUT receiver when actuated by acoustic signal generated from a PMUT transmitter.

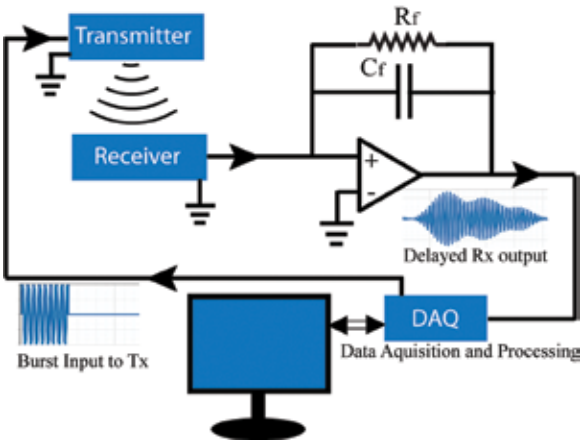

Figure 12. Electronic integration and proximity sensing setup.

PMUT cell was generally less than 50 µV. Moreover, this electrical output was very noisy and susceptible to electromagnetic radiation noise if an unshielded transmitter was brought close to the receiver.

In order to sense this small voltage output, a charge pre-amplifier circuit was employed (Figure 12). A Charge amplifier uses a feedback capacitor with an ultralow noise operational amplifier. It gives a low impedance voltage output proportional to the charge generated by the receiver and scaled by the ratio of the sensor capacitance to the feedback capacitance. The transmitter and receiver were packaged in metallic blocks in order to avoid electromagnetic noise.

We used a high frequency data acquisition system (PCI-6115) supplied by National Instruments and Labview graphical programming interface for complete integration of the PMUT. A burst signal with 20 cycles per burst at resonant frequency was generated by the DAQ and applied across the transmitter to generate acoustic signal. When received on the receiver, it generated charge which was fed to the charge pre-amplifier. The pre-amplifier output was then sent back to DAQ system, wherein it was filtered in a narrow range of the operating frequency and further processed to read the delay time between the transmitted burst and the received burst (Figure 13). This delay was used to estimate the distance between the transmitter and the receiver. With this configuration, we were able to use the PMUT as a proximity sensor, using a single element as transmitter and another element as receiver, for up to 10 cm.

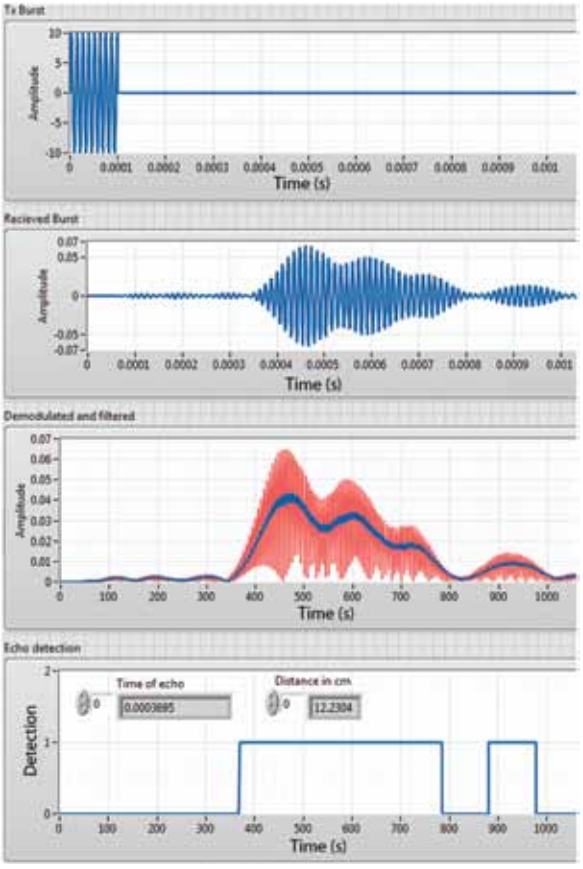

Figure 13. Signal processing and distance estimation.

6 Conclusions

We have reported successful fabrication and electronic integration of a Piezoelectric Micromachined Ultrasonic Transducers. The PMUT devices show the first resonance peak in 72–78 kHz frequency range. Through further characterization we have established that the deflection sensitivity of PMUT is approximately 0.8 µm = V which corresponds to 57 dB SPL at 1 m distance for the device actuated at 1 V. Further, the PMUT has been integrated with electronics and used as a proximity sensor. Signal conditioning of receiver output has been done using a charge amplifier. With this setup, we could use a PMUT cell as a proximity sensor up to 10 cm distance.

Acknowledgement

We gratefully acknowledge the Center for Development of Advanced Computing (C-DAC), Thiruvananthapuram, for funding this project under the ASTec program of the MCIT.

References

Arya Yahspal, Maters Thesis. (2009) *Design, Fabrication and Testing of a Piezoelectric Micromachined Ultrasonic Sensor*, Indian Institute of Science, Bangalore.

Bu, Minqiang., Melvin, T., Ensell, G., Wilkinson, J.S. and Evans, A.G.R. (2003) Design and theoretical evaluation of a novel microfluidic device to be used for PCR. *J Micromech Microeng*. **13**, S125–S130.

Damjanovic, D., Mayergoyz, I. and Bertotti, G. (2005) *Hysteresis in Piezoelectric and Ferroelectric Materials*, The Science of Hysteresis, Volume 3, Elsevier 2005.

Dixit, P. and Miano, J. (2006) *Effect of SF6 flow rate on the etched surface profile and bottom grass formation in deep reactive ion etching process*, Journal of Physics: Conference Series 34, pp. 577582.

http://www.murata.com/enlobal/products/sensor/ultrasonic

Khuri-Yakub, B.T., Degertekin, F.L., Jim, X-C., Calms, S., Ladabam, L., Hansen, S. and Zhang, X.J. (1998) *Silicon Micromachined Ultrasonic Transducers*, IEEE Ultrasonics Symposium pp. 985–991.

Kinsler, L.E., Frey, A.R., Coppens, A.B., and Sanders, J.V. (2000) *Fundamentals of Acoustics* 4th Edition, John Wiley and Sons, Inc.

Lu, Y., Tang, H., Fung, S., Tsai, J.M., Daneman, M., Boser, B.E. and Horsley, D.A. (2015) Waveguide piezoelectric micromachined ultrasonic transducer array for short-range pulse-echo imaging. *Appl Phys Lett*. **106**, 193506.

Lu, Y., Tang, H., Fung, S., Wang, Q., Tsai, J M., Daneman, M., Boser, B.E., and Horsley, D.A. (2015) Ultrasonic fingerprint sensor using a piezoelectric micromachined ultrasonic transducer array integrated with complementary metal oxide semiconductor electronics. *Appl Phys Lett*. **106**, 263503.

Muralt, P., Ledermann, N., Bab, J., Barzegar, A., Gentil, S., Belgacem, B., Petitgrand, S., Bosseboeuf, A., and Setter, N. (2005) *Piezoelectric Micromachined Ultrasonic Transducers Based on PZT Thin Films*, IEEE transactions on ultrasonics, ferroelectrics, and frequency control. **52**, (12).

Olfatnia, M., Xu, T., Ong, L.S., Miao, J.M., and Wang, Z.H. (2010) Investigation of residual stress and its effects on the vibrational characteristics of piezoelectric-based multilayered microdiaphragms. *J Micromech Microeng*. **20**.

Prasad, S.A.N., Gallas, Q., Horowitz, S., Homeijer, Brian., Sankar, B.V., Cattafesta, L.N., and Sheplak, M. (2006) Analytical Electroacoustic Model of a Piezoelectric Composite Circular Plate. *AIAA Journal*. **44**, (10).

Przybyla, R.J., Shelton, S.E., Guedes, A., Izyumin, I., Kline, M.H., Horsley, D.A. and Boser, B.E. (2011) In-air rangefinding with an AlN piezoelectric

micromachined ultrasound transducer. *IEEE Sensors Journal*. **11**, 2690–2697.

Przybyla, R.J., Tang Hao, Guedes, A., Shelton, S., Horsley, D. and Boser, B.E. (2015) 3D Ultrasonic Rangefinder on a Chip. *IEEE Journal of Solid-State Circuits*. **50**.

Sammaoura Firas, Smyth Katherine, Bathrust Stephen., and Kim, S.G. (2012) *An Analytical Analysis of the Sensitivity of Circular Piezolelelctric Maicromachined Transducer to Residual Stress*, IEEE International ULtrasonics Symposium Proceedings.

Senturia S. (2001) *Microsystem Design*. Kluwer Academic Publishers.

Wah, Thein. (1962) *Vibrations of Thin Plates*. Journal of Acoustical Society of America.

Yamashita, K., Katata, H., Okuyama, M., Miyoshi, H., Kato, G., Aoyagi, S. and Suzuki, Y. (2002) Ultrasonic micro array sensors using piezoelectric thin films and resonant frequency tuning. Sensors and Actuators A 97–98, pp. 302–307.

Ajay Dangi received his B. Tech. degree in Mechanical Engineering from Indian Institute of Technology, Banaras Hindu University, Varanasi, in 2010. He worked as an engineer in petroleum industry from 2010 to 2011. He is currently pursuing Ph.D. in Mechanical Engineering at Indian Institute of Science, Bangalore. His research interests include design and fabrication of MEMS sensors, nonlinear dynamics, vibrations, and acoustics.

Amod Hulge received his B. Engg. degree in Production Engineering from University of Pune, in 2003. He received his M.S. degree in 2009 in Mechanical Engineering from Swiss Federal Institute of Technology, Zurich (ETHZ). He worked as a Project Associate at Indian Institute of Science. He is currently working as a consultant engineer for various manufacturing related industries.

Anish S. obtained a Bachelors degree in Instrumentation Engineering from Cochin University of Science and Technology in the year 1999 and a Masters degree in Industrial Power and Automation from the National Institute of Calicut in the year 2012. He is currently working as the Senior Engineer in the Centre for Development of Advanced Computing (CDAC), Thiruvananthapuram, a Scientific Society of the Ministry of Communication and Information Technology, Government of India. His research interests include industrial control system engineering and design, sensor electronics for MEMS, process modelling and simulation.

Dr. S. Rominus Valsalam graduated in Mathematics from the Madurai University in 1977. He received his B.Tech degree in Instrument Technology from the Madras Institute of Technology, Anna University, Chennai in 1980, M.S Degree in Control Engineering from the Indian Institute of Technology, Chennai in 1989 and Ph.D Degree in Adaptive Optimal Control from the Anna University, Chennai in 2003. He is currently working as the Associate Director and Head of the Department of Control and Instrumentation in the Centre for Development of Advanced Computing (CDAC), Thiruvananthapuram, a Scientific Society of the Ministry of Communication and Information Technology, Government of India. He is also a faculty member for the M.Tech Programme in VLSI and Embedded Systems at the ER&DCI Institute of Technology, CDAC, Thiruvananthapuram. He has published 50 papers in International and National journals and conferences. His research interests include Process Modelling, Optimization, Digital Signal Processing, MEMS/ Nano Technology, Kalman Filtering, State Estimation and Prediction, Adaptive Optimal Control, Neuro-Fuzzy-Genetic Intelligent System technologies, Data Fusion, Machine Learning. He is a Senior Member of IEEE and fellow of The Institution of Engineers (India). He has filed patent applications for five inventions, out of which one patent has been awarded and the other four are under the review process.

Prof. Rudra Pratap received a B.Tech. degree from the Indian Institute of Technology, Kharagpur, India, in 1985, a Masters degree in mechanics from the University of Arizona, Tucson, in 1987, and a Ph.D.

degree in Theoretical and Applied Mechanics from Cornell University, Cornell, NY, in 1993. He taught at the Sibley School of Mechanical and Aerospace Engineering, Cornell University during 1993–1996, prior to joining the Indian Institute of Science in 1996. He is currently a Professor with the Department of Mechanical Engineering and the Centre for Nano Science and Engineering, Indian Institute of Science Bangalore, India. His research interests include MEMS design, computational mechanics, nonlinear dynamics, structural vibration, and vibroacoustics.